

# Internal stress and strain in heavily boron-doped diamond films grown by microwave plasma and hot filament chemical vapor deposition

W. L. Wang,<sup>a)</sup> M. C. Polo, G. Sánchez, J. Cifre, and J. Esteve  
*Departament Física Aplicada i Electrònica, Universitat de Barcelona, Av. Diagonal 647,  
E-08028 Barcelona, Spain*

(Received 20 November 1995; accepted for publication 6 May 1996)

The internal stress and strain in boron-doped diamond films grown by microwave plasma chemical vapor deposition (MWCVD) and hot filament CVD (HFCVD) were studied as a function of boron concentration. The total stress (thermal+intrinsic) was tensile, and the stress and strain increased with boron concentration. The stress and the strain measured in HFCVD samples were greater than those of MWCVD samples at the same boron concentration. The intrinsic tensile stress, 0.84 GPa, calculated by the grain boundary relaxation model, was in good agreement with the experimental value when the boron concentration in the films was below 0.3 at. %. At boron concentrations above 0.3 at. %, the tensile stress was mainly caused by high defect density, and induced by a node-blocked sliding effect at the grain boundary. © 1996 American Institute of Physics. [S0021-8979(96)10915-4]

## I. INTRODUCTION

The internal stress in diamond thin films, as in many other thin film materials,<sup>1-6</sup> accumulated either during or after deposition, has a significant effect on their physical properties. The films with tensile stress will tend to split and spall, and compressive films can be peeled off from the substrate and delaminate. These stress states will result in a deterioration of the mechanical properties of the films if the strain energy in the film is greater than the interfacial energy between it and the substrate.

To design useful chemical vapor deposition (CVD) diamond materials and understand its reliability issues, the internal stress in the diamond films has been a subject of expanding interest and investigation in recent years.<sup>7-11</sup> For example, Knight and White<sup>12</sup> reported diamond film stresses of 5.5 GPa (compressive) on alumina and 2.1 GPa (tensile) on WC. Windischmann *et al.*<sup>13</sup> studied the stress in the diamond films produced by MWCVD, and found that internal stress is highly sensitive to the deposition conditions; tensile or compressive total stresses can be achieved depending on the methane fraction and deposition temperature. Wang *et al.*<sup>14</sup> elucidated the relationship between internal stress and grain size formed by dc plasma CVD. Sails *et al.*<sup>15</sup> reported stress in  $\langle 100 \rangle$ ,  $\langle 110 \rangle$ , and  $\langle 111 \rangle$  oriented diamond films using Raman spectroscopy. Chiou *et al.*<sup>16</sup> determined the internal stress of CVD diamond films by the bending beam technique and from the width of the x-ray diffraction peak. Their results indicate that the compressive stress can be partly released by improving the diamond crystallinity of the films, for example, by the addition of argon at higher concentration of CH<sub>4</sub>/H<sub>2</sub>. As mentioned above, these studies are mainly focused on undoped CVD diamond films on Si (polycrystalline growth) or *c*-BN (epitaxial growth). These internal stresses depend mainly on the nondiamond carbon phases and the hydrogen incorporated in the films under various

deposition conditions, and thus predominantly exhibit a compressive component.

High stress in doped diamond films can cause stress-induced transport phenomena in semiconductor devices. To date, no stress measurements in doped diamond films have been reported. In this work, we have studied the internal stress and strain in boron-doped polycrystalline diamond films grown on Si(111) by both hot filament CVD (HFCVD) and microwave plasma CVD (MWCVD) using Raman spectroscopy. The experiments were performed at room temperature on films with different boron concentrations. The origin of the measured stress is also discussed in this article.

## II. EXPERIMENT

The diamond films used in this study were prepared by HFCVD and MWCVD. The reaction gases were a mixture of CH<sub>4</sub> and H<sub>2</sub>. The boron source was trimethylboron B(CH<sub>3</sub>)<sub>3</sub> (TMB) diluted in helium at 0.5 vol %. The diamond films were deposited onto polished *p*<sup>+</sup> silicon substrates, which had been scratched with 1 μm diamond powder and cleaned in a methanol ultrasonic bath. In the hot filament system, reaction gases were activated by a folded tungsten filament with a diameter of 1 mm and 150 mm long. The filament was heated to 2000 °C in a methane atmosphere until its full carburization. The substrates were placed on a graphite holder, 2 cm from the filament. In a tubular microwave reactor, the gases were activated in a 600 W microwave plasma, and the substrates were placed in a graphite holder at the center of the waveguide. In both deposition processes, the total gas pressure was fixed at 4500 Pa, the substrate temperature at 920 °C, and the CH<sub>4</sub> concentration (in H<sub>2</sub>) at 1%. The TMB–helium volume ratio in the reaction gas was in the range from 0% to 4.5%.<sup>17</sup>

The quality of the films was characterized by Raman spectroscopy, electron microscopy, scanning electron microscopy (SEM) and transmission electron microscopy (TEM)] and x-ray diffraction (XRD). The boron content and its distribution in the films were measured by wavelength-

<sup>a)</sup>Permanent address: Department of Physics, Lanzhou University, Lanzhou 73000, P.R. China.

dispersive electron probe x-ray microanalysis and secondary ion mass spectrometry.<sup>18</sup>

Raman spectra were measured at room temperature with 514.5 nm of an argon ion laser focused onto the films with an objective lens of 0.8 aperture. The laser spot size on the films was about 1  $\mu\text{m}$ . The laser light was incident normal to the surface, and scattered light was collected in 180° scattering geometry. Most measurements were made at 1  $\text{cm}^{-1}$  resolution, but some were made with 0.5  $\text{cm}^{-1}$  resolution. The sample could be moved in two dimensions with a translation stage.

### III. RESULTS

Raman spectroscopy is used to analyze internal stress of boron-doped diamond films. Raman spectroscopy can provide a qualitative account of the components of a diamond film and gives an indication of the inherent stress and crystallinity. The optical-phonon band of diamond at 1332  $\text{cm}^{-1}$  is very sensitive to applied stress. Raman shifts around 3  $\text{cm}^{-1}$  caused by a stress of 1 GPa (Ref. 19) have been reported. The Raman diamond peak shifts to higher and lower frequency under compressive and tensile stresses, respectively.<sup>20</sup> Earlier stress investigations of diamond films using Raman spectroscopy were based on a biaxial stress model developed originally to study the stress in Si(100) grown epitaxially on sapphire.<sup>10,14</sup> Recently, Ager III *et al.*<sup>21</sup> proposed a quantitative measurement of residual biaxial stress by Raman spectroscopy in polycrystalline diamond films. By assuming the presence of biaxial stresses, the degree of stress can be estimated from the following equation for the singlet phonon:<sup>21</sup>

$$\sigma = -1.08 \text{ GPa/cm}^{-1} \Delta\nu, \quad (1)$$

where  $\Delta\nu$  is the shift of the Raman peak of diamond films with respect to that of natural diamond. The minus and plus signs are assigned to compressive and tensile stresses, respectively. The strain of the diamond films can also be calculated from the relation,  $e = (S_{11} + S_{12})\sigma$ , where  $S_{11}$  and  $S_{12}$  are the diamond elastic compliance constants, and  $S_{11} = 9.524 \times 10^{-14} \text{ cm}^2/\text{dyn}$ ,  $S_{12} = -0.9913 \times 10^{-14} \text{ cm}^2/\text{dyn}$ , respectively.

The Raman spectra of a series of films with various boron concentrations are shown in Fig. 1. Figures 1(a) and 1(b) represent HFCVD samples and MWCVD samples, respectively. For boron contents up to 0.3 at.%, Raman spectra revealed that the films were mainly diamond crystals, as evidenced by the sharp 1332  $\text{cm}^{-1}$  peak. In addition, a broad band appeared centered at around 1550  $\text{cm}^{-1}$ , which was attributed to disordered graphic phases. To determine the contributions of diamond and disordered graphitic phase to the total Raman scattered light, Raman spectra were deconvoluted using Gaussian curves, whose position, width at half-maximum, and amplitude were variable parameters. Three different contributions were needed to fit the broad 1550  $\text{cm}^{-1}$  band: the D and G peak of polycrystalline graphite at around 1345 and 1560  $\text{cm}^{-1}$ , and a low intensity band centered approximately at 1470  $\text{cm}^{-1}$  attributed to a tetrahedrally bonded diamond precursor.<sup>22</sup> The amount of diamond

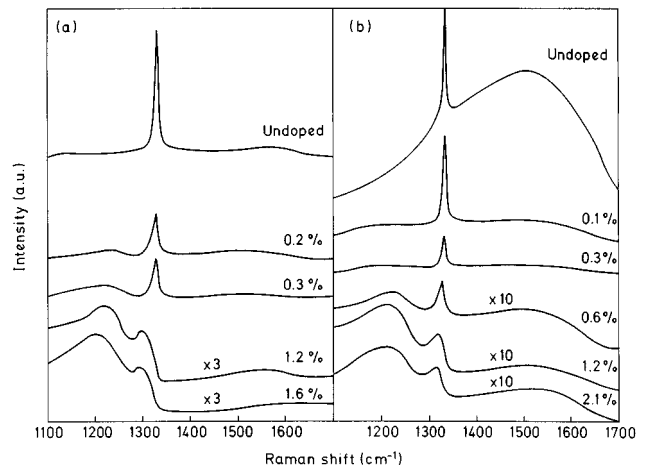


FIG. 1. Raman spectra of a series of diamond films obtained by (a) HFCVD and (b) MWCVD, with different boron concentration.

in the films can be calculated by a relative Raman cross section of diamond to graphite of 1/50 (Ref. 23) as follows:

$$C_d = 100A_d / \left( A_d + \frac{\sum A_i}{50} \right), \quad (2)$$

where  $A_d$  and  $A_i$  are the area of the fitted curves corresponding to the 1332  $\text{cm}^{-1}$  diamond peak and the graphitic bands, respectively. Figure 2 shows the relative amount of diamond as a function of boron content. In MWCVD films, the amount of diamond increased from 75% in the undoped sample to 98% in the doped sample with boron of 0.3 at.%, but in HFCVD samples the improvement was slight because the undoped sample already had a diamond phase of 90%.

The changes of Raman spectra were similar for both sets of samples when boron contents were higher than 0.3 at.%. The diamond peak broadened and shifted to lower wave numbers and its relative intensity also decreased. Moreover, a broad band appeared centered at 1200  $\text{cm}^{-1}$  attributed to nanocrystalline diamond<sup>24</sup> and increased with increasing boron concentration.

Figure 3 shows the dependence of the measured total stress (thermal+intrinsic) on the boron concentration in the films from 0.1 to 2.1 at.%. Figures 3(a) and 3(b) illustrate

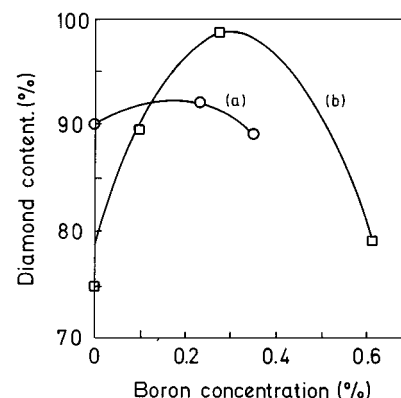


FIG. 2. The relative amount of diamond as a function of boron content: (a) HFCVD; (b) MWCVD. The lines are a guide for the eye.

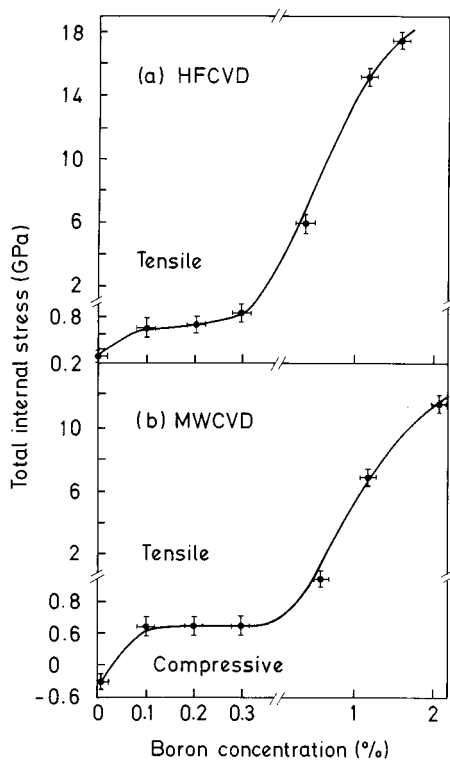


FIG. 3. The dependence of the measured total stress on boron concentration in the diamond films produced by (a) HFCVD and (b) MWCVD. The lines are a guide for the eye.

HFCVD and MWCVD samples. The uncertainty in the stress measurement is about  $\pm 10\%$ . The total stress in both sets of samples was tensile with a maximum of 18 GPa at boron concentration of 1.6 at. % for the HFCVD sample, and increased with boron concentration. Over the boron doping range studied, the films were verified to be diamond by x-ray diffraction, electron diffraction, and Raman spectroscopy. For the undoped sample grown by MWCVD, the stress was compressive, but in the HFCVD sample it was tensile, and both were much lower than in doped samples. The tensile stress increased drastically at boron concentrations above 0.3 at. %, and the stress in HFCVD samples was always greater than that in MWCVD samples.

In heavily boron-doped diamond films obtained by CVD, an impurity band is formed and a metalliclike conductivity is observed. In addition, at very high doping levels, the Fano interaction occurs owing to quantum mechanical interference between the Raman phonon and transitions from the broadened impurity band to continuum states.<sup>25–28</sup> The Raman peak centered at  $1332\text{ cm}^{-1}$  shifted to lower frequencies with increasing boron doping, which may be caused by a combination of the self-energy shift due to the Fano interaction and tensile stress in the lattice from the incorporation of substantial quantities of boron. Ager III *et al.*<sup>28</sup> reported in a recent article that the Fano line shapes were formed at doping levels of about  $10^{21}\text{ cm}^{-3}$ . In our experiment, the Fano line shapes were found above 0.3 at. % boron concentration (about  $10^{21}\text{ cm}^{-3}$ ) according to fitting calculation.<sup>26</sup> Therefore, the actual stress value in the films was lower than the measured values as boron concentration rose above 0.3 at. %.

The thermal stress  $\sigma_{\text{th}}$  was calculated as follows:

$$\sigma_{\text{th}} = [E/(1-\nu)] \int_{T_1}^{T_2} (a_s - a_f) dT, \quad (3)$$

where  $a_f$  and  $a_s$  are the expansion coefficient of diamond and silicon, respectively,  $E/(1-\nu)$  is the biaxial Young's modulus, e.g., 1345 GPa for diamond,<sup>29</sup>  $T_1$  is temperature during the deposition and  $T_2$  is room temperature. The calculated thermal stress of diamond films deposited at  $920\text{ }^\circ\text{C}$  was compressive with a value of 0.21 GPa.

The intrinsic stress  $\sigma_{\text{in}}$  was calculated from

$$\sigma_{\text{in}} = \sigma_t - \sigma_{\text{th}}, \quad (4)$$

where  $\sigma_t$  is the measured total stress. The intrinsic stress was therefore tensile in the boron content range studied. For example, the total stress  $\sigma_t$  of HFCVD and MWCVD samples was about 0.65 GPa at 0.2 at. % B, so the intrinsic stress was 0.86 GPa.

The strain behavior with increasing boron content was the same as that of the stress, e.g., the strain increased with boron concentration. The maximal strain was about 1.56% at a boron concentration of 1.6 at. % for the HFCVD sample, slightly greater than that of the MWCVD samples.

From XRD analysis it was observed that the lattice constant tended to stretch with increasing boron concentration (Fig. 4), as evidenced by the increase in the tensile stress caused by boron content in the films. The increase in the lattice constant in HFCVD samples was higher than that of MWCVD samples, since the tensile stress in HFCVD samples was greater than that in MWCVD samples. In addition, an average grain size of about 150 nm, determined by a contribution of SEM images and XRD data, was found for samples with boron contents up to 0.3 at. %, but at higher boron concentrations, the grain size decreased. Thus, for samples with boron contents of 2 at. % the average value of the grain size was about 40 nm.

#### IV. DISCUSSION

Generally speaking, compressive intrinsic stress in the films is attributed to impurities, whereas defects such as vacancies, dislocation, or grain boundaries produced tensile stress.<sup>30–32</sup> In undoped diamond films, the nondiamond carbon phase and hydrogen are assumed to be responsible for compressive stress,<sup>33–35</sup> and the grain boundary relaxation is the origin of tensile intrinsic stress.<sup>13</sup> Our experimental results have shown that the stress in boron-doped diamond films is tensile, and enhanced with increasing boron concentration. Thus the origin of the tensile stress needs to be explained.

The lattice constant of the diamond is  $3.567\text{ \AA}$ , and that of silicon  $5.430\text{ \AA}$ . The lattice may expand in the diamond layers and shrink in the silicon because of the lattice mismatch if the diamond film is deposited on the silicon substrate. Consequently, diamond films on silicon substrates should be under a tensile stress. However, this stress is distributed only near the interface between the films and substrate. Besides, the incorporation of substantial quantities of boron in the films results in a lattice expansion of diamond.

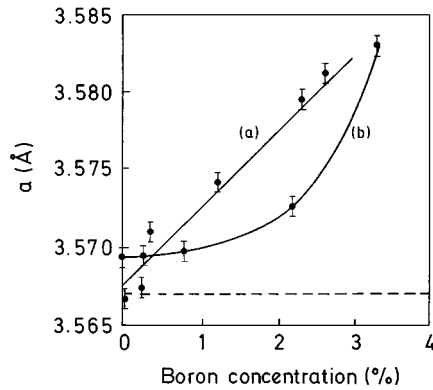


FIG. 4. Relationship between lattice constant and boron content in the diamond films grown by (a) HFCVD and (b) MWCVD. The dotted line denotes the lattice constant of natural diamond. The continuous lines are a guide for the eye.

For boron doping levels higher than 2 at.%, the lattice expansion is greater as shown in Fig. 4. Therefore, the stress caused by the lattice mismatch is weaker in the doped films.

The polycrystalline diamond films consist of fine crystallites, and the films contain a high density of grain boundaries and voids. The attractive atomic forces acting across grain boundaries or micropore gaps induce an elastic strain in the anchored grain due to a constrained relaxation, e.g., the grain boundary relaxation process.<sup>13,36</sup> The average grain size decreased with increasing boron concentration. The grain size is much smaller in heavily doped samples, which implies a high grain boundary density in the films. Common grain boundary relaxation modes also include those of slacking disorder, low-index asymmetric facets, and microfacets which are related to the short-range nature of the interatomic interaction. The relaxation strength of the grain boundary varies with the number of disordered groups and the degree of disorder of each group. The intrinsic tensile stress caused by the grain boundary relaxation can be estimated from the following relationship:<sup>37</sup>

$$\sigma = [E/(1 - \nu)] \delta/d, \quad (5)$$

where  $\delta$  is the constrained relaxation of the lattice constant and has a value of 0.077 nm for diamond,<sup>13</sup> and  $d$  is the crystal size. The intrinsic tensile stress with an average grain size of 120 nm is about 0.84 GPa, according to Windischmann *et al.*'s calculation.<sup>13</sup> This stress value agrees with our measured values when the boron concentration is below 0.3 at.%. For instance, the intrinsic tensile stress of both HFCVD and MWCVD samples is about 0.86 GPa at boron concentration of 0.2 at.%. However, the calculated stress values are lower than the measured values as boron concentration is higher than 0.3 at.% (see Fig. 3). This is due to complicated stress mechanisms produced in the heavily doped diamond films.<sup>38</sup>

At higher boron doping levels, the interstitial boron incorporation in the lattice or boron precipitation at the grain boundary starts to occur. Thus, the usual grain boundary relaxation can be decreased or suppressed by the impurity atoms. Mitsuhashi *et al.*<sup>39</sup> reported Raman spectroscopy analyses which revealed that the full width at half-maximum

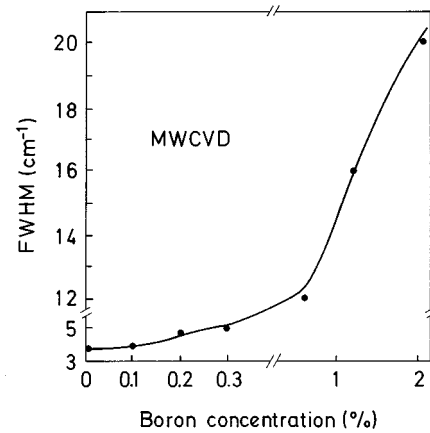


FIG. 5. Influence of the boron content on the FWHM of Raman line in the diamond films prepared by MWCVD. The line is a guide for the eye.

(FWHM) of the  $1332 \text{ cm}^{-1}$  band increased from  $1.76$  to  $2.16 \text{ cm}^{-1}$  as the dislocation density increased from  $4.0 \times 10^4$  to  $3.3 \times 10^5 \text{ cm}^{-2}$  on the surface of electron-assisted CVD diamond films on (100) diamond substrates.<sup>39</sup> Our experimental results showed that the maximum value of FWHM is about  $18 \text{ cm}^{-1}$  with a boron concentration of 1.6 at.% for MWCVD samples as shown in Fig. 5. This suggests that there is an extremely high dislocation density in the films. The dislocations are mainly concentrated on the grain boundaries,<sup>37</sup> which promotes the grain boundary relaxation. High defect density in the films involving dislocations and vacancies, easily gliding and moving along grain boundaries, can develop tensile stress. On the other hand, the FWHM of HFCVD samples was greater than that of MWCVD samples (not shown). This implies that HFCVD samples contain many more defects. Thereby, the stress and strain of HFCVD samples were greater than those of MWCVD samples (see Fig. 3). The enormous differences of the defect density between high and low boron doped films cause the stress in HFCVD films not to be linearly dependent on the boron concentration although the lattice constant in these samples almost linearly increased with boron concentration (see Fig. 4) owing to its main dependence on the grain size.

In addition, nanocrystalline diamond phase formation was enhanced when the boron concentration was higher than 0.3 at.%. The complicated nanocrystalline grain boundaries contained many defects and the impurities can easily slide during film deposition at substrate temperature above  $850 \text{ }^\circ\text{C}$ . The grain boundary sliding is opposed by the boundary grain. The opposition develops an internal stress, which eventually stops the sliding. The internal stress also acts on the grain. The sliding is not only blocked by the grain on a boundary, but is also restricted by the boundary nodes (triple points). The blocking of sliding by the nodes produces an additional internal stress in the grain free area of a boundary. This is referred to as an internal stress induced by node-blocked grain boundary sliding.<sup>40-42</sup> At substrate temperature above  $850 \text{ }^\circ\text{C}$ , boron diffusion, coalescence of vacancies, and formation of voids may relax the internal stress. A slight decrease in the stress because of the diffusional relax-

ation causes further sliding, which increases the internal stress.

The films tend to generate strain or distortion under stress, whereas the strain and distortion can relax the stress. The stress and strain will reach a stable state when their energies are in equilibrium state. The films are spalled or peeled off if the strain energy exceeds the interface energy between the film and substrate and among the grains.

## V. SUMMARY

The internal stress and strain in boron-doped diamond films deposited by MWCVD and HFCVD are investigated as a function of boron concentration. The total stress is tensile, and stress and strain are enhanced with increasing boron concentrations. The tensile stress is explained in terms of the grain boundary relaxation model due to the short-range nature of interatomic interaction when boron concentration in the films is below 0.3 at. %. In heavily boron-doped diamond films (>0.3 at. %), the origin of internal stress is mainly attributed to high defect density, and is induced by the blocking of grain boundary sliding.

## ACKNOWLEDGMENT

This work has been financially supported by the Comisión Interministerial de Ciencia y Tecnología of the Spanish Government under Contract No. MAT93-CO3-O2.

- <sup>1</sup>W. A. P. Claassen, *Thin Solid Films* **129**, 239 (1985).
- <sup>2</sup>J. C. Angus, C. C. Hayman, and R. W. Hoffman, *Proc. SPIE* **969**, 2 (1988).
- <sup>3</sup>F. M. d'Heurle and J. M. E. Harper, *Thin Solid Films* **1716**, 81 (1989).
- <sup>4</sup>W. L. Wang and K. J. Liao, *Thin Solid Films* **165**, 173 (1988).
- <sup>5</sup>H. Windischmann, R. W. Collins, and J. M. Cavese, *J. Non-Cryst. Solids* **85**, 261 (1986).
- <sup>6</sup>L. Pkanevicius, K.-F. Bodowi, N. Durand, J. Delafond, and Ph. Goudeau, *Surf. Coat. Technol.* **71**, 254 (1995).
- <sup>7</sup>J. A. Baglio, B. C. Farnsworth, S. Hankin, G. Hamil, and D O'Neil, *Thin Solid Films* **212**, 180 (1992).
- <sup>8</sup>B. S. Berry, W. C. Pritchett, J. J. Cuomo, C. R. Guarnieri, and S. J. Whitehair, *Appl. Phys. Lett.* **57**, 3021 (1990).
- <sup>9</sup>W. L. Wang, K. J. Liao, and Y. J. Gao, *Phys. Status Solidi* **126**, K115 (1991).
- <sup>10</sup>M. Yoshikama, H. Ishida, A. Ishitani, T. Murakami, S. Koizumi, and T. Inuzuka, *Appl. Phys. Lett.* **57**, 428 (1990).

- <sup>11</sup>H. Windischmann and K. J. Gray, *Diam. Relat. Mater.* **4**, 837 (1995).
- <sup>12</sup>D. S. Knight and W. B. White, *J. Mater. Res.* **4**, 385 (1989).
- <sup>13</sup>H. Windischmann, G. F. Epps, Y. Cong, and R. W. Collins, *J. Appl. Phys.* **69**, 2231 (1991).
- <sup>14</sup>W. L. Wang, K. J. Liao, J. Y. Gao, and A. M. Liu, *Thin Solid Films* **215**, 174 (1992).
- <sup>15</sup>S. R. Sails, D. J. Gardiner, and M. Bowden, *Appl. Phys. Lett.* **65**, 43 (1994).
- <sup>16</sup>Y. H. Chiou, C. T. Hwang, M. Y. Han, J. H. Jou, Y. S. Chang, and H. C. Shih, *Thin Solid Films* **253**, 119 (1994).
- <sup>17</sup>J. Cifre, J. Puigdollers, M. C. Polo, and J. Esteve, *Diam. Relat. Mater.* **3**, 628 (1994).
- <sup>18</sup>M. C. Polo, J. Cifre, J. Puigdollers, and J. Esteve, *Thin Solid Films* **253**, 136 (1994); J. Cifre, F. Lopez, J. L. Mornza, and J. Esteve, *Diam. Relat. Mater.* **500**, 1 (1992).
- <sup>19</sup>H. Boppert, J. V. Straaten, and I. F. Silvera, *Phys. Rev. B* **32**, 1423 (1985).
- <sup>20</sup>M. Yoshikawa, G. Katagiri, H. Ishida, A. Ishitani, M. Ono, and K. Matsumara, *Appl. Phys. Lett.* **55**, 2608 (1989).
- <sup>21</sup>J. W. Ager III and M. D. Drory, *Phys. Rev. B* **48**, 2601 (1993).
- <sup>22</sup>W. A. Yarbrough and R. Roy, *Diamond and Diamond-like Materials*, edited by G. H. Johnson, A. R. Badzian, and M. W. Geis (Materials Research Society, Pittsburgh, PA, 1988), Vol. EA-15, Extended abstracts, p. 33.
- <sup>23</sup>N. Wada and S. A. Solin, *Physica B&C* **105**, 353 (1981).
- <sup>24</sup>R. J. Nemanich, J. T. Glass, G. Lucovsky, and R. E. Shroder, *J. Vac. Sci. Technol. A* **6**, 1783 (1988).
- <sup>25</sup>D. Naraducci, C. R. Guarnieri, and J. J. Cuomo, *J. Electrochem. Soc.* **138**, 2446 (1991).
- <sup>26</sup>U. Fano, *Phys. Rev.* **124**, 1886 (1961).
- <sup>27</sup>F. Cerdeira, T. A. Fjeldly, and M. Cardona, *Phys. Rev. B* **8**, 47374 (1973).
- <sup>28</sup>J. W. Ager III, W. Walukiewicz, M. Meluskey, M. A. Plano, and M. I. Landstrass, *Appl. Phys. Lett.* **66**, 616 (1995).
- <sup>29</sup>*The Properties of Diamond*, edited by J. E. Field (Academic, London, 1979).
- <sup>30</sup>J. Priost, H. L. Caswell, and Y. Buda, *Vacuum* **12**, 391 (1962).
- <sup>31</sup>K. Ozawa, N. Takagi, and K. Asama, *Jpn. J. Appl. Phys.* **22**, 767 (1983).
- <sup>32</sup>W. L. Wang and K. J. Liao, *Acta Phys. Sin.* **36**, 1529 (1987).
- <sup>33</sup>C. C. Chiu, Y. Liou, and Y. D. Yuang, *Thin Solid Films* **260**, 118 (1995).
- <sup>34</sup>K. H. Chen, Y. L. Lai, J. C. Lin, J. J. Song, L. C. Chen, and C. Y. Houn, *Diam. Relat. Mater.* **4**, 460 (1995).
- <sup>35</sup>W. L. Wang and K. J. Liao, *Acta Phys. Sin.* **41**, 1906 (1992).
- <sup>36</sup>J. D. Finegan and R. W. Hoffman, AECC Technical Report No. 18, Case Institute of Technology, 1961.
- <sup>37</sup>G. B. Olson and M. Cohen, *Acta Metal.* **27**, 1907 (1979).
- <sup>38</sup>S. A. Lgon, R. J. Nemanich, N. M. Johnson, and D. K. Biegelsen, *Appl. Phys. Lett.* **40**, 316 (1982).
- <sup>39</sup>M. Mitsuhashi, S. Karasawa, S. Ohya, and F. Togoshi, *Appl. Surf. Sci.* **60/61**, 565 (1992).
- <sup>40</sup>R. Monzen and T. Mori, *Scr. Metall. Mater.* **39**, 1009 (1994).
- <sup>41</sup>R. Monzen and T. Mori, *Acta Metall.* **43**, 1451 (1995).
- <sup>42</sup>R. Monzen, K. Kitagawa, and T. Mori, *Acta Metall.* **37**, 1619 (1989).